Journal of Materials Chemistry B

Accepted Manuscript

This article can be cited before page numbers have been issued, to do this please use: X. Liu, Q. Huang, C. Yang, Q. Zhang, W. Chen, Y. Shen and M. Sui, *J. Mater. Chem. B*, 2016, DOI: 10.1039/C6TB02262F.

ROYAL SOCIETY OF CHEMISTRY

rsc.li/materials-b

View Article Online
DOI: 10.1039/C6TB02262F

Multi-stimuli Responsive Nanoparticulate SN38 Prodrug for Cancer Chemotherapy

Xun Liu,[a,b※] Qian Huang,[a,b※] Caixia Yang,[a,b,c] Qianzhi Zhang,[a,b] Wan Chen,[a,b] Youqing Shen,[a] Meihua Sui [b,a,]*

[a] *College of Chemical and Biological Engineering, Zhejiang University, Hangzhou, China, 310027;*

[b] *Center for Cancer Biology and Innovative Therapeutics, Key Laboratory of Tumor Molecular Diagnosis and Individualized Medicine of Zhejiang Province, Clinical Research Institute, Zhejiang Provincial People's Hospital, Hangzhou, China, 310014;*

[c] *ACEA BIO(Hangzhou) Co. LTD, Hangzhou, China, 310030*

[*]Corresponding author at the Center for Cancer Biology and Innovative Therapeutics, Key Laboratory of Tumor Molecular Diagnosis and Individualized Medicine of Zhejiang Province, Clinical Research Institute, Zhejiang Provincial People's Hospital, Hangzhou, 310014, China.

E-mail address: suim@zju.edu.cn (M. Sui)

[※] equal contribution for the first two authors.

Keywords: nanocarrier; stimuli-sensitive; PEG; SN38; CPT-11

View Article Online
DOI: 10.1039/C6TB02262F

Abstract:

Modification of drug delivery system (DDS) with stimuli-responsive elements could significantly increase the tumor-specific delivery of anticancer drugs. Herein we synthesized a novel multiple stimuli-responsive SN38 prodrug, named as PEG-S-S-SN38, through conjugating PEG (MW: 2000) and SN38 with disulfide bond and carbonic ester linkage as the linkers for efficient delivery of SN38. The amphiphilic PEG-S-S-SN38, with a high SN38 loading content, could self-assemble into nanoparticles (NPs) with a stable diameter of ~73 nm. PEG-S-S-SN38 NPs release SN38 very slowly in physiological pH, while quickly release SN38 in the presence of GSH, esterase and H_2O_2, all of which are abundant in the cytoplasm of cancer cells. PEG-S-S-SN38 NPs could be quickly internalized into tumor cells, achieve vesicular escape and nuclear localization, and exhibit remarkable *in vitro* anticancer activity similar to SN38. Encouragingly, PEG-S-S-SN38 NPs exhibit the same effects on cell cycle regulations as SN38 *in vitro*. Most importantly, the inhibition rate of tumor growth induced by PEG-S-S-SN38 NPs in a xenograft tumor model reached 72.49% ± 6.26%, which was nearly double that of the corresponding clinical drug CPT-11 (38.64% ± 13.04%) at a dosage equivalent to 10 mg kg^{-1} SN38. Our data suggest that the multi-stimuli responsiveness of PEG-S-S-SN38 NPs remarkably enhances their therapeutic activity against heterogeneous or mixed cell population in tumors, making this new DDS a promising alternative of CPT-11 for cancer treatment.

View Article Online
DOI: 10.1039/C6TB02262F

Introduction

The clinical application of anticancer drugs is often restricted by multiple factors, for instance, low solubility or stability, lack of selectivity to tumor tissues or tumor cells, which result in decreased therapeutic activity and severe side effects. Formulation strategies such as nanoparticle-based drug delivery systems (DDS) have emerged as the most promising technology to increase drug solubility or stability, improve pharmacokinetics, increase the passive targeting ability of carried drugs by the enhanced permeability and retention effect (EPR).[1-3] Moreover, modification of DDS with specific stimuli-responsive elements or with active targeting ligands (*e.g.*, folic acid) further increases the tumor-specific drug delivery and retention.[4]

CPT-11 (irinotecan) is a widely used chemotherapeutic drug to treat a range of cancers. However, it needs to be converted to 7-ethyl-10-hydroxy-camptothecin (SN38), which has 100-1000 fold higher cell-killing potency than CPT-11, before exhibiting significant anti-cancer effect.[5-7] Unfortunately, the conversion rate of CPT-11 to SN38 in cancer patients is only around 2-8% after CPT-11 infusion, with great interindividual difference, leading to significant interpatient variability in clinical responses.[8,9] CPT-11 may also cause severe gastrointestinal toxicity and myelosuppression.[10] Therefore, direct administration of SN38 would bring more clinical advantages and may prevent the side effects of CPT-11. As SN38 has very low solubility in all kinds of pharmaceutically acceptable solutions, considerable interests have been focused on the development of DDS for targeted delivery of SN38.[11-14] However, some significant limitations are related with the SN38-delivering DDS reported in the literature, *e.g.* low drug loading and unfavorable release profile.[11, 15] For example, polymer conjugate of SN38 EZN-2208 has a payload of only 3.7% even though four SN38 moleculars were conjugated to the PEG backbone.[15]

Stimuli-sensitive anticancer DDS, through responses to either an internal physiopathologic changes (pH, redox potential, *etc.*) or external stimulus (temperature, magnetic field, *etc.*), could achieve targeted delivery, controlled release and accumulation of drug at tumor sites.[16-19] For instance, the intracellular redox potential contains 100-1000 times higher concentration of reducing

View Article Online
DOI: 10.1039/C6TB02262F

glutathione (GSH) tripeptide than extracellular environment. Moreover, the levels of GSH in tumor tissues are at least 4-fold higher than those in normal tissues.[20-22] As disulfide bonds are stable in extracellular space with low concentration of GSH, while could be quickly degraded in a highly reductive intracellular environment, redox-responsive delivery systems containing disulfide bonds have attracted much attention for targeted delivery of bioactive molecules for both therapeutics and diagnosis.[23, 24] Disulfide bonds may be incorporated in the backbones, side chains, cross-linkers of polymeric carriers, or directly used for conjugation of anticancer drug (*e.g.* doxurobucin, cisplatin and camptothecin) with the polymer backbone.[25-29] Another strategy to design stimuli-responsive DDS is based on enzymatic responsiveness that has multiple advantages including high selectivity, substrate specificity and mild operating condition, *e.g.* ester bonds for esterase-catalyzed bioconversion.[30, 31] Encouragingly, novel dual and multi-stimuli responsive delivery systems that respond to a combination of two or more stimulus have recently been developed and further improved the performances of DDS.[32]

Through using a hydrophobic drug as the hydrophobic part of the block copolymer, we recently established a self-assembling prodrug strategy to prepare nano-vehicles for delivery of several anticancer drugs, which has shown additional advantages over traditional DDS.[33-35] Herein, for the first time, we successfully synthesized a novel multiple stimuli-responsive nanocarrier, named as PEG-S-S-SN38, through conjugating PEG and SN38 with both disulfide bonds and carbonic ester linkage as the linkers (Scheme 1). PEG (MW: 2000) was selected as the hydrophilic part to improve the biocompatibility of the nanoparticles and prolong their circulation in blood.[36] This novel system was carefully characterized and its biological effects were investigated using a series of assays. Our data demonstrated that P EG-S-S-SN38 nanoparticles possess significant superiority and may become a promising alternative of CPT-11 for cancer treatment.

View Article Online
DOI: 10.1039/C6TB02262F

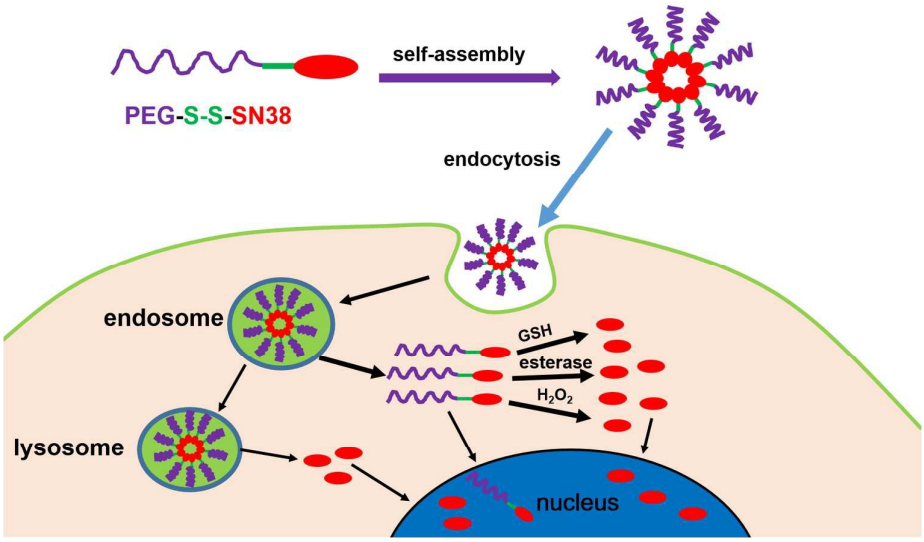

Scheme 1. Illustration of the formation, cellular internalization, distribution and multi-stimuli responsive drug release of PEG-S-S-SN38 nanoparticles. The amphiphilic PEG-S-S-SN38 prodrug could self-assemble into nanoparticles. The obtained PEG-S-S-SN38 nanoparticles invaginate and pinch off of the plasma membrane to form endocytic vesicles, followed by a fraction of vesicles containing nanoparticles fusing with lysosomes. After vesicular escape (*e.g.* endosomal and lysosomal escape), the internalized nanoparticles could be quickly degraded in the presence of GSH, esterase and H_2O_2, leading to controlled release of active SN38 to target nucleus.

Experimental

Chemicals, cell cultures and mice

Chloromethyl methyl ether (98%) (MOM-Cl) was purchased from Xiya Reagent (Chengdu, China). N,N-Diisopropylethylamine (DIPEA), 4-dimethylaminopyridine (DMAP) and bis(trichloromethyl)carbonate (BTC) were purchased from Energy Chemical (Shanghai, China). 7-ethy-10-hydroxyl-camptothecin (SN38) was purchased from Sendflld Science and Technology (Xi'an, China). Irinotecan hydrochloride was purchased from Chengdu Yuancheng Biotechnology (Chengdu, China). Bis(2-hydroxyethyl) disulfide (ca. 50% in water) was purchased from Tokyo Chemical Industry (Tokyo, Japan).

BCap37 (human breast cancer), MCF-7 (human breast cancer) and its multidrug resistant (MDR) subline MCF-7/ADR, KB (human epidermoid cancer) and its MDR subline KBv200,

View Article Online
DOI: 10.1039/C6TB02262F

SKOV3 (human ovarian cancer), LoVo (human colon cancer) and Vero (monkey fibroblast-like kidney cell) cell lines are maintained in our laboratory and have been used in our previous studies. Cancer cell lines were incubated in either RPMI1640 or DMEM supplemented with 10% heat-inactivated fetal bovine serum (FBS), penicillin (100 units mL^{-1}) and streptomycin (100 μg mL^{-1}) in a humidified atmosphere of 5% CO_2 at 37°C. Both culture medium and fetal serum were purchased from Genom Biological Technology (Hangzhou, China). The 6-8-week-old female BALB/c homozygous athymic nude mice were purchased from the Animal Center of Zhejiang Academy of Medical Sciences, and maintained under standard conditions. All animal studies were approved by the Animal Care and Use Committee of Zhejiang University and Zhejiang Academy of Medical Sciences.

Synthesis of MOM-SN38

SN38 (2 g) was dissolved in 20 mL CH_2Cl_2 and 4.46 mL DIPEA, then 1.93 mL MOM-Cl was added into the mixture with stirring. After stirring for 24 h at room temperature, the mixture was filtered. The solid was purified by passing through a column chromatography packed with silica gel (eluent MeOH/CH_2Cl_2=3/97), and pure MOM-SN38 was obtained and characterized by ^{1}H NMR spectroscopy and High Performance Liquid Chromatography (HPLC).

Synthesis of MOM-SN38-S-S-OH

MOM-SN38 (0.7 g) was mixed with DMAP (0.63 g) in 70 mL dry CH_2Cl_2, and BTC (0.18 g) was added into the solution under argon atmosphere. The reaction was allowed to proceed at room temperature for 30 mins, then 15 mL THF solution containing dry bis(2-hydroxyethyl) disulfide (2.47 g) was injected under argon atmosphere. After stirring for 24 h at room temperature, the solution was washed with HCl aqueous solution (pH 3.0) and saturated $NaHCO_3$ aqueous solution successively. After evaporation of the solvent, the product was purified by passing through a column chromatography packed with silica gel (eluent MeOH/ CH_2Cl_2=2/98), and the pure MOM-SN38-S-S-OH obtained was characterized by ^{1}H NMR spectroscopy and HPLC.

Synthesis of PEG-S-S-SN38

View Article Online
DOI: 10.1039/C6TB02262F

MOM-SN38-S-S-OH (0.45 g) was mixed with DMAP (0.29 g) in 70 mL dry CH_2Cl_2, and BTC (74 mg) was added into the solution under argon atmosphere. The reaction was allowed to proceed at room temperature for 30 mins, then the solution of 10 mL dry CH_2Cl_2 containing $mPEG_{2000}$ (0.7 g) was added dropwise into the solution with stirring in the ice bath. After stirring for 48 h at room temperature, the solvent was evaporated and the residue was dialyzed for 5 days against DMSO refreshed every 24 h. After further dialysis against water to remove DMSO, the purified product was obtained after freeze drying and characterized by ^1H NMR spectroscopy and HPLC.

Preparation of PEG-S-S-SN38 nanoparticles (NPs) and stability measurement

10 mg PEG-S-S-SN38 was dissolved in 2 mL DMSO. The solution was added dropwise into 10 mL deionized water with stirring, followed by dialysis against deionized water and concentrated to a final SN38 concentration of 1 mg mL^{-1}. The size and size distribution of the nanoparticles were measured using dynamic light scattering (DLS, Malvern Zen3600, UK) and the morphology of the nanoparticles was observed by transmission electron microscopy (TEM). Furthermore, a certain amount of FBS was added into 1 mL of the above solution at the final concentration of 40% to investigate the stability of PEG-S-S-SN38 NPs. The samples were tested by DLS at 2.5 h, 6 h and 32 h respectively.

Determination of the critical micelle concentration (CMC)

A known amount of nile red solution in CH_2Cl_2 was added to a series of vials to give a final concentration of 1×10^{-6} M. After CH_2Cl_2 was evaporated, 10 mL of a series of measured amount of PEG-S-S-SN38 solution was added to each vial, and the solution was stirred overnight in darkness. The fluorescence emission intensity of each solution was determined at the wavelength of 650 nm (exited at 540 nm) using a microplate reader. CMC was obtained as the intersection of the tangents to the two linear portions of the graph of the fluorescence intensity as a function of PEG-S-S-SN38 concentration.

Measurement of SN38 release

View Article Online
DOI: 10.1039/C6TB02262F

The PEG-S-S-SN38 NPs (equivalent to 200 μg mL^{-1} SN38) were prepared in PBS and incubated at 37°C. At timed intervals, 100 μL solution was withdrawn for HPLC test. The MOM-SN38 concentration was calculated using a relative method from the total peak area of the absorbance at 360 nm. The MOM-SN38 release in the presence of GSH (or esterase, H_2O_2) was carried out in the same method except adding each agent to the solution to give the final concentration stated.

Cellular uptake and subcellular distribution

The cellular uptake, accumulation and internalization of different formulations of SN38 were monitored by confocal laser scanning microscopy (CLSM, Nikon-A1, Japan) and flow cytometric analysis (FACS, Becton Dickinson FACS Calibur, USA). To visualize cells using CLSM, cells were cultured on glass-bottomed petri dishes for 24 h before treatment. 3,3′-dioctadecyloxacarbocyanine perchlorate (DIO) staining solution at a final concentration of 5 μM was then added into the dishes for 20 mins to label cell membrane. Afterwards, the solution was replaced with fresh medium containing PEG-S-S-SN38 NPs (equivalent to 10 μg mL^{-1} SN38) for designated time points. In another two experiments, after the treatment of PEG-S-S-SN38 NPs, tumor cells cultured in petri dishes were incubated with either LysoTracker green (Molecular Probes, USA) at a concentration of 200 nM for 1.5 h to label lysosomes, or DRAQ5 at a concentration of 5 μM for 20 mins to label nucleus. DIO for cell membrane and LysoTracker green for lysosomes were observed using a 488 nm laser, and the emission wavelength was read from 500 to 550 nm and shown as green. PEG-S-S-SN38 was observed using a 405 nm laser, and the emission wavelength was read from 425 to 475 nm and shown as red. DRAQ5 for nucleus was observed using a 640 nm laser, and the emission wavelength was read from 662 to 737 nm and shown as blue.

For flow cytometric analysis, tumor cells plated in 6-well plates were treated with nile red-loaded PEG-S-S-SN38 NPs (equivalent to 0.04 μg mL^{-1} SN38) for 1 h, 2 h and 6 h at 37° C, respectively. Then the cells were collected and rinsed twice with cold PBS. Finally, the cells were dispersed in cold PBS again and subjected to flow cytometric analysis with the excitation set to be FL2

View Article Online
DOI: 10.1039/C6TB02262F

(488 nm).

3-(4,5-dimethylthiazol-2-yl)-2,5-diphenyltetrazolium bromide (MTT) assay and xCELLigence system real time cellular analysis (RTCA)

The *in vitro* anticancer activity of CPT-11, SN38 and PEG-S-S-SN38 NPs was determined by 48 h-MTT assay in multiple cell lines including MCF-7, MCF-7/ADR, KB, KBv200, BCap37 and SKOV3, according to the methods described previously.[32, 34] The absorbance in each individual well was determined at 562 nm with a microplate spectrophotometer (SpectraMaxM2E, Molecular Devices, USA). Each drug concentration was tested in triplicate and in three independent experiments. Moreover, as a complementary method of MTT assay, xCELLigence RTCA MP system (ACEA Biosciences, USA) was used to evaluat the cytotoxicity of CPT-11, SN38 and PEG-S-S-SN38 NPs in LoVo and Vero cells. In brief, LoVo and Vero cells were seeded into the E-plates 96 at 1.5×10^6 cells per well and 3.0×10^6 cells per well, respectively, and incubated for 24 h. Then cells were administered with designated concentrations of CPT-11, SN38 and PEG-S-S-SN38 NPs respectively and monitored for at least 72 h. The normalized cell index were calculated according to RTCA-integrated software (ACEA Biosciences, USA).

Analysis of cell cycle and apoptosis

After the treatment of CPT-11, SN38 and PEG-S-S-SN38 NPs, at an equivalent SN38 concentration of 0.04 μg mL^{-1} for 24 h and 48 h, respectively, cell samples were prepared according to the Cell Cycle and Apoptosis Analysis Kit (Beyotime Biotechnology, China). In brief, at the end of each time point, tumor cells were collected and fixed in 70% cold ethanol diluted in PBS. After rinsed with cold PBS, cell samples were incubated in water bath at 37°C in darkness, with each sample containing 0.5 mL buffer solution, 25 μL propidium iodide solution and 10 μL RNase. Finally, the samples were examined using FACScan and the obtained data were processed with Modifit LT 3.2 Software.

In vivo antitumor studies

View Article Online
DOI: 10.1039/C6TB02262F

In vitro cultured BCap37 cells were collected and washed with PBS, then implanted into the right flanks of nude mice (1×10^6 cells). When the tumor volumes were around 90 mm^3, mice were randomly divided into three groups (n=6 per group): (a) CTL (PBS), (b) irinotecan (equivalent to 10 mg kg^{-1} SN38) and (c) PEG-S-S-SN38 (equivalent to 10 mg kg^{-1} SN38). The treatment regimens were initiated on day 1 (*i.v.*), repeated every 3 days for a total of 6 cycles. The body weight of each animal and the tumor size ([major axis]×[minor axis]^2×1/2) were measured before each intravenous injection. Three days after the last treatment, animals were sacrificed following institutional guidelines. The curve of tumor growth was drawn based on tumor volume (mm^3) and corresponding time (days) after the first treatment. Inhibition rates (IR) of tumor growth were calculated using the following formula: IR= (mean tumor weight of control group – mean tumor weight of experimental group)/mean tumor weight of control group×100%. Tumors were resected, weighed, and fixed in formalin for paraffin embedding, followed by preparation of tissue sections and staining with hematoxylin and eosin for histological examinations. The *in vivo* proliferation of tumor cells was studied by immunohistochemistry staining for proliferation marker Ki-67 (Beijing Zhongshan Golden Bridge Biotechnology, China) in BCap37 xenograft tumors and counterstained with hematoxylin.

Statistical analysis

Data are presented as means±standard errors. Tumor volumes over time were analyzed by one-way ANOVA (analysis of variance) and subsequently by Student's *t*-test. All other statistical analyses were performed using Student's *t*-test. Differences were considered statistically significant at a level of $P<0.05$.

Results and discussion

Synthesis and characterization of SN38 prodrug and PEG-S-S-SN38 NPs

The design and synthesis route for a new SN38 prodrug, named as PEG-S-S-SN38, is shown in Figure 1A. SN38 has a C_{20} alcoholic hydroxyl group and a C_{10} phenolic hydroxyl group. The C_{20}

View Article Online
DOI: 10.1039/C6TB02262F

alcoholic hydroxyl group, along with the lactone ring and pyridone group, are essential for the topoisomerase inhibitory activity of SN38, while the presence of the α-OH group at the C_{20} chiral centre facilitates the hydrolysis of the lactone ring. Herein, we first protected the C_{10} phenolic hydroxyl group with chloromethyl methyl ether using N,N-Diisopropylethylamine as a catalyst in CH_2Cl_2 to obtain MOM-SN38. Next, the reaction of C_{20} alcoholic hydroxyl group of MOM-SN38 with BTC and bis(2-hydroxyethyl) disulfide in the presence of DMAP afforded MOM-SN38-S-S-OH. Finally, the prodrug PEG-S-S-SN38 was obtained through the reaction of MOM-SN38-S-S-OH with $mPEG_{2000}$ using BTC in the presence of DMAP as the catalyst. The structures and purity of MOM-SN38, MOM-SN38-S-S-OH and PEG-S-S-SN38 were confirmed by NMR (see Supporting Information, Figure S1-S3) and HPLC (Figure S4). As determined with DLS and TEM, the amphiphilic PEG-S-S-SN38, with a SN38 loading content as high as 15 wt%, could self-assemble into nanoparticles with a diameter of about 73 nm in PBS (Figure 1B). Further studies indicated that PEG-S-S-SN38 NPs have good stability, with the size only slightly increased even after 32 h incubation with 40% FBS (Figure S5). The appropriate size of PEG-S-S-SN38 NPs and their favorable stability may increase the targeting ability of nanocarriers through EPR effect, and prevent sequestration by reticuloendothelial system (RES), both of which leading to the effective accumulation of nanoparticles into tumor tissues. Moreover, the CMC of PEG-S-S-SN38 in aqueous solution was 53 $\mu g\ mL^{-1}$ (Figure S6).

Multi-stimuli responsive release of SN38 from PEG-S-S-SN38 NPs

The release of SN38 from PEG-S-S-SN38 NPs was detected by HPLC. As shown in Figure 1C, PEG-S-S-SN38 NPs released SN38 very slowly in PBS at pH 7.4, without the phenomenon of initial burst release and with only 11.3% of SN38 released after 48 h of incubation. However, in the presence of 10 mM GSH, these NPs quickly hydrolyzed and up to 91.3% of SN38 was released

View Article Online
DOI: 10.1039/C6TB02262F

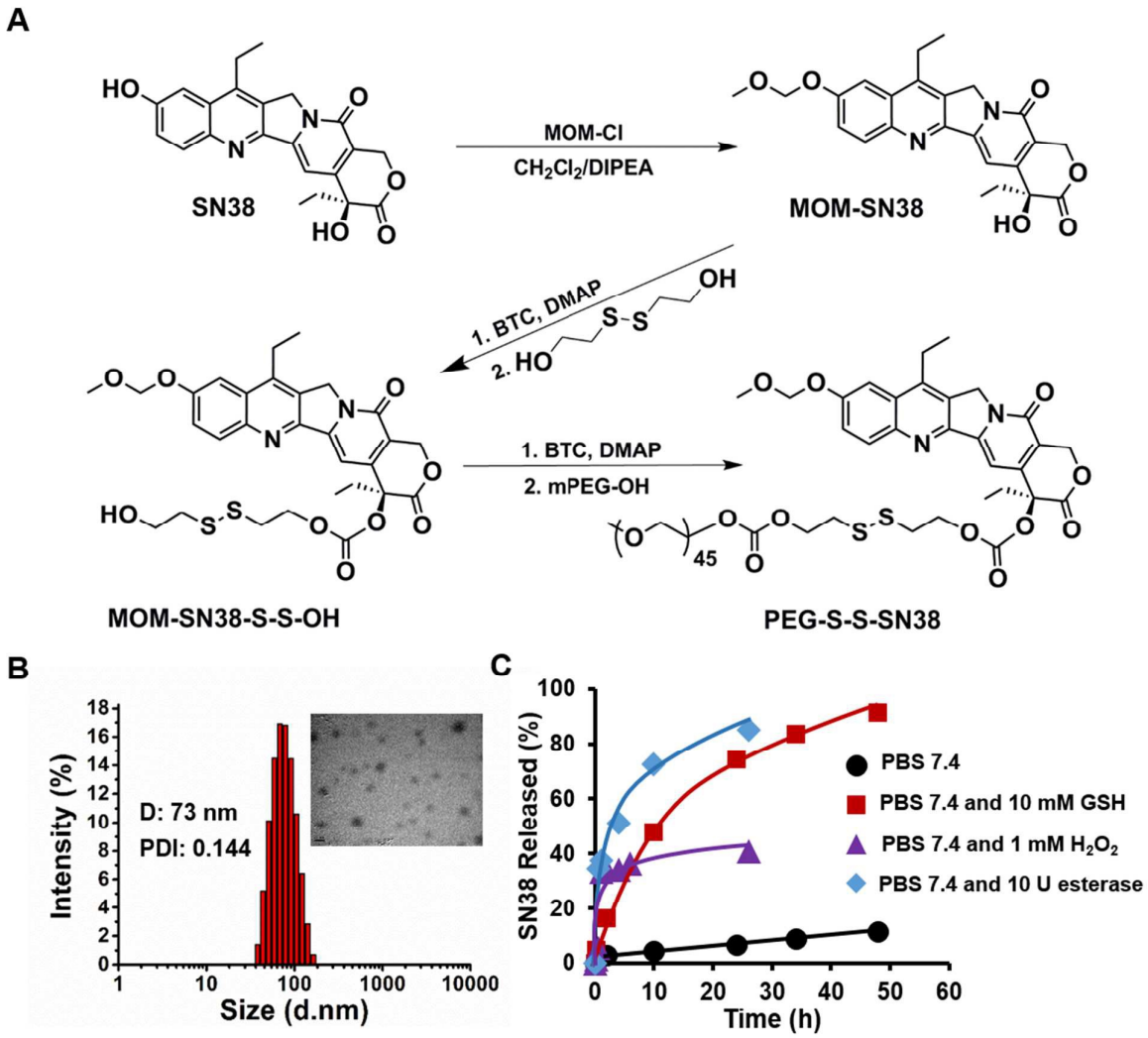

Figure 1. Synthesis and characterization of SN38 prodrug PEG-S-S-SN38. (A) Synthesis route of PEG-S-S-SN38 prodrug. (B) The size distribution of PEG-S-S-SN38 nanoparticles determined by DLS and the morphology of PEG-S-S-SN38 nanoparticles observed by TEM (insert, scale bar=100 nm). (C) SN38 release kinetics from PEG-S-S-SN38 nanoparticles in PBS at pH 7.4 and in the presence of 10 mM GSH, 10 U esterase and 1 mM H_2O_2.

after 48 h of incubation, indicating that the fast SN38 release could be triggered by reduction with GSH. Meanwhile, in the presence of esterase, which is abundant in cytoplasm, up to 85% of SN38 was released from PEG-S-S-SN38 NPs after 26 h of incubation. This data coincides with our anticipation that the carbonic ester linkage between PEG and SN38 could be easily cleaved when exposed to intracellular esterase. In some ways, this esterase-responsive property of PEG-S-S-SN38 is

View Article Online
DOI: 10.1039/C6TB02262F

superior to the carboxylesterase-responsiveness of CPT-11 because of the remarkable interspecies and individual variability of carboxylesterase. Interestingly, we further found that in the presence of 1 mM H_2O_2, one of the intracellular prevailing reactive oxygen species (ROS) overproduced in cancer cells compared with normal cells, PEG-S-S-SN38 could also be quickly hydrolyzed and effectively release SN38. This accelerated drug release might be caused by the oxidation of the disulfide bonds in the presence of high level of ROS. These data demonstrates that for the first time, through conjugating PEG and SN38 with both disulfide bond and carbonic ester linkages, we have successfully obtained a triple-stimuli responsive nanoparticulate SN38 prodrug to achieve better controlled release of SN38.

Cellular uptake and subcellular distribution of PEG-S-S-SN38 NPs

When observed with CLSM (Figure 2A-J), PEG-S-S-SN38 NPs exhibited red fluorescence excited at 405 nm. It is worth mentioning that the absorption spectrum of free SN38 is 360 nm and the emission wave is 530 nm. Therefore, no red fluorescence would be observed with 405 nm excitation if free SN38 was released from PEG-S-S-SN38 NPs. Herein, lipophilic carbocyanine dyes DIO, LysoTracker green and DRAQ5 were used to label cell membrane (green in Figure 2A-D), lysosomes (green in Figure 2E-H) and nucleus (blue in Figure 2I-J), respectively.

As shown in Figure 2A-D, exposure to PEG-S-S-SN38 NPs resulted in a significant time-dependent accumulation of SN38 in BCap37 cells via endocytosis, as indicated by endocytic internalization of the plasma membrane and the co-localization of drug and membrane (shown as yellow). After incubation for 30 mins, a large amount of PEG-S-S-SN38 NPs had been trapped in endocytic vesicles (shown as yellow, Figure 2C), followed by most of the nanoparticles escaped from the vesicles at 2 h (Figure 2D, shown as the reduced yellow fluorescence). Interestingly, data presented in Figure 2E-H revealed that most PEG-S-S-SN38 NPs were not co-localized with lysosomes at these time points. This phenomena might be attributed to the occurrence of fast vesicular escape of PEG-S-S-SN38 NPs into cytosol, which preventing the further transportation of nanopar-

View Article Online
DOI: 10.1039/C6TB02262F

ticles into the lysosomes. Encouragingly, after 6 h of incubation, some PEG-S-S-SN38 NPs entered the cell nuclei (shown as pink in Figure 2I-J). These findings demonstrate that PEG-S-S-SN38 NPs could be quickly internalized into tumor cells, achieve vesicular escape and nuclear localization. Moreover, the cellular uptake of PEG-S-S-SN38 NPs was also monitored by flow cytometry. As summarized in Figure 2K, these nanoparticles quickly entered into BCap37 cells, with rates as high as 50.4%, 70.1% and 89.6%, respectively, after 1 h, 2 h, and 6 h of incubation, which was consistent with the data obtained with CLSM.

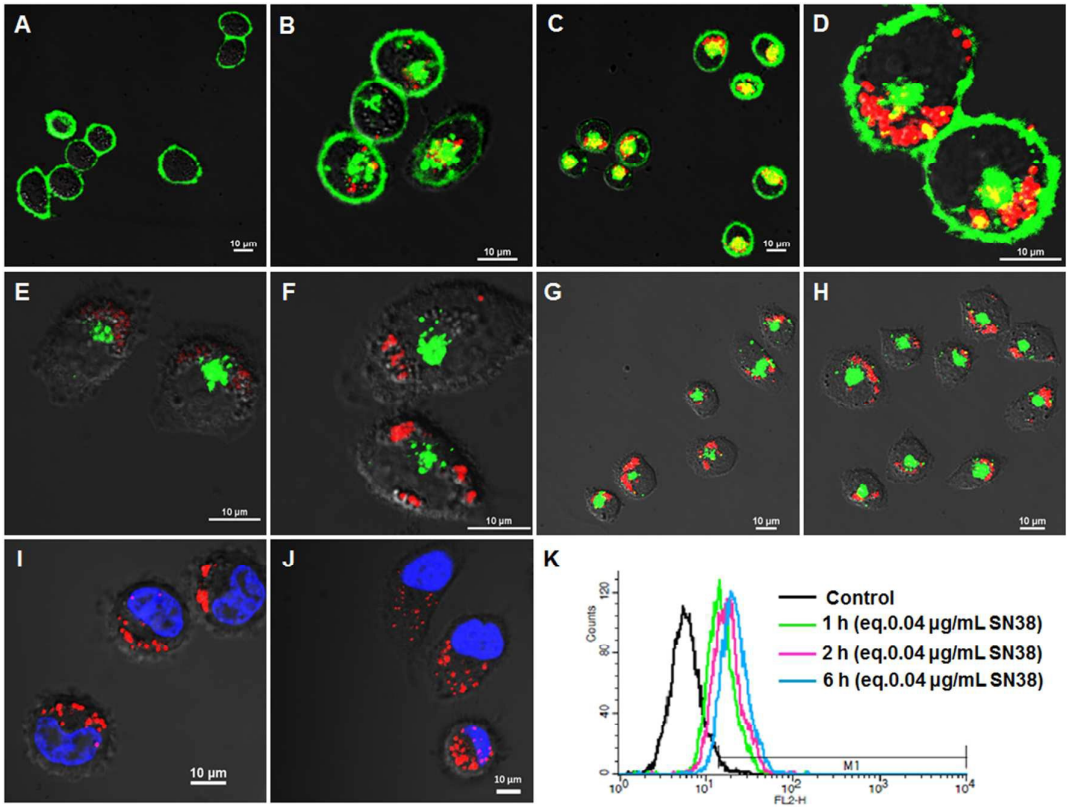

Figure 2. Cellular uptake and subcellular localization of PEG-S-S-SN38 nanoparticles in BCap37 cells as observed with CLSM. A-D, images were taken after incubation with PEG-S-S-SN38 for 0 min (A), 10 mins (B), 30 mins (C) and 120 mins (D), respectively. Cell membrane was labeled with lipophilic carbocyanine dyes DIO (shown as green), and PEG-S-S-SN38 were shown as red. E-H, images were taken after incubation with PEG-S-S-SN38 for 10 mins (E), 30 mins (F), 60 mins (G) and 120 mins (H), respectively. Lysosomes were labeled with LysoTracker green (shown as green), and PEG-S-S-SN38 were shown as red. I-J, observation of the nuclear localization after incubation with PEG-S-S-SN38 for 2 h (I) and 6 h (J), respectively. Cell nucleus was labeled with DRAQ5 (shown as blue), and PEG-S-S-SN38 was shown as red. K, cellular uptake of PEG-S-S-SN38 nanoparti-

View Article Online
DOI: 10.1039/C6TB02262F

cles into BCap37 cells after incubation for 0 h, 1 h, 2 h and 6 h, respectively, as determined by flow cytometric analysis. A-J, scale bar=10 μm; PEG-S-S-SN38 at a concentration equivalent to 10 μg mL^{-1}SN38.

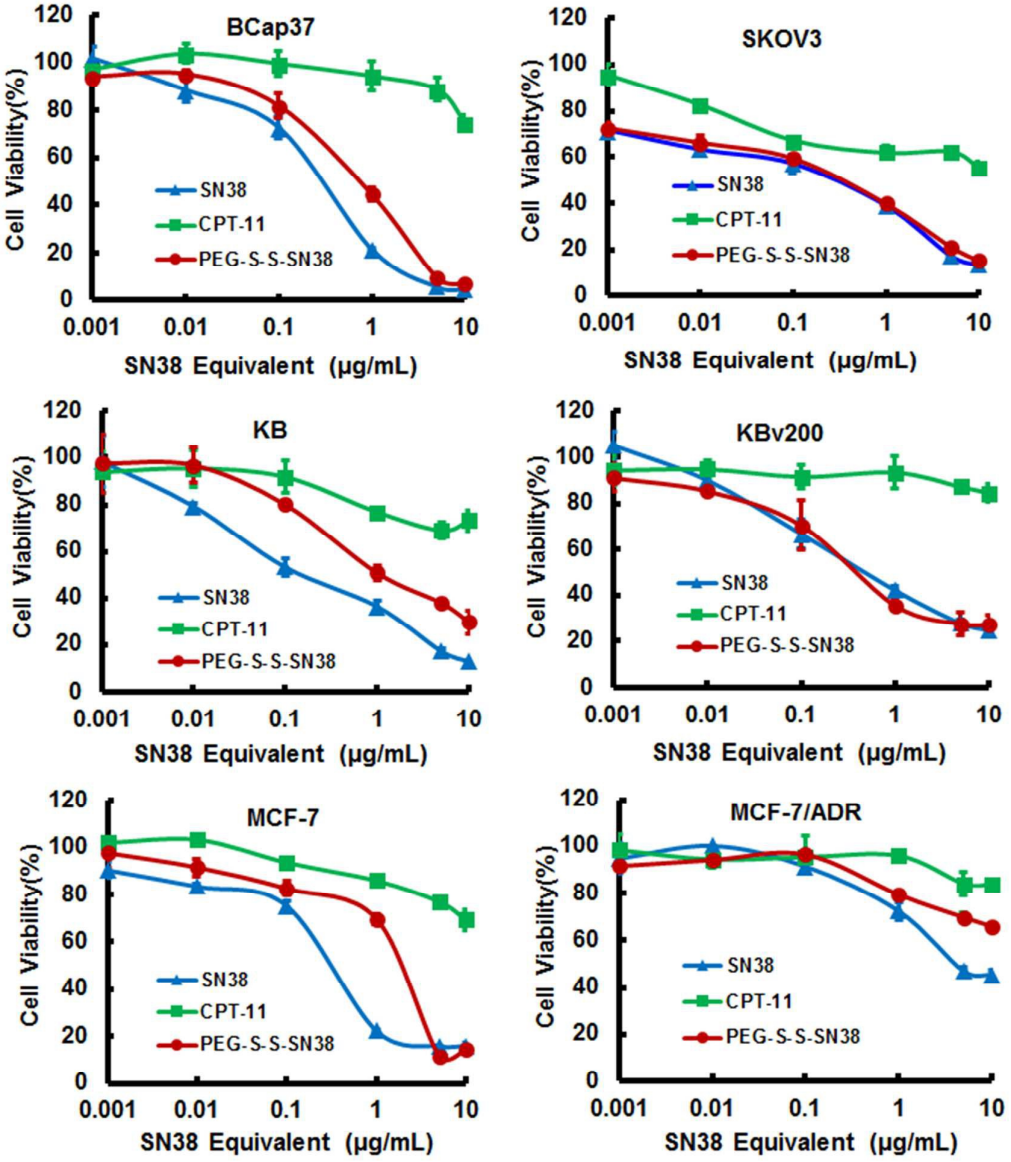

Figure 3 *In vitro* cytotoxicity of CPT-11, SN38 and PEG-S-S-SN38 NPs in BCap37, SKOV3 and other two pairs of parental sensitive and MDR cancer cell lines (KB and KBv200; MCF-7 and MCF-7/ADR) after 48 h incubation with equivalent CPT-11, SN38 and PEG-S-S-SN38 NPs.

In vitro cell-killing activity of CPT-11, SN38 and PEG-S-S-SN38 NPs

The *in vitro* cell-killing activity of PEG-S-S-SN38 NPs, in comparison with CPT-11 and free SN38, was evaluated with MTT assays (Figure 3) and RTCA (Figure S7). Our data showed that

View Article Online
DOI: 10.1039/C6TB02262F

CPT-11 had little cytotoxicity against all these cell lines, while PEG-S-S-SN38 NPs exhibited similar dose-dependent and comparable anticancer activity as SN38 in most tested cancer cell lines (Figure 3). These data indicates that the multi-stimuli responsiveness enables PEG-S-S-SN38 NPs efficiently release active SN38 after taken up by cancer cells, which is critical for their cell-killing activity. In RTCA assays, PEG-S-S-SN38 NPs also produced significant *in vitro* cell-killing activity comparable to free SN38, which was much higher than that of CPT-11 in both LoVo and Vero cells (Figure S7).

Cell cycle regulations induced by CPT-11, SN38 and PEG-S-S-SN38 NPs

Cell cycle distribution of BCap37 cells exposed to CPT-11, SN38 and PEG-S-S-SN38 NPs, at a concentration equivalent to 0.04 μg mL^{-1} SN38, were monitored by flow cytometry (Figure 4). It is known that SN38, a topoisomerase I inhibitor, can induce irreversible double-chain DNA damage, thereby resulting in cell cycle arrest at S and G2/M phases or even inducing cell death. Indeed, our data showed that BCap37 cells were arrested at S phase after 24 h of incubation with 0.04 μg mL^{-1} SN38 (percent of S phase: 90.35%), which progressed to G2 phase arrest at 48 h (percent of G2 phase: 99.70%). Encouragingly, PEG-S-S-SN38 NPs at the equivalent SN38 concentration exhibited exactly the same effects on cell cycle changes as SN38 (with 90.58% S-phase cells at 24 h and 96.14% G2-phase cells at 48 h, respectively), indicating that PEG-S-S-SN38 NPs could quickly enter into cells and release active SN38 effectively. It is worth mentioning that in our previous report, the regulatory effect of OEG-SN38, a prodrug prepared through attaching oligo (ethylene glycol) (OEG) to SN38 *via* ester bond at the C_{20} position, on the cell cycle arrest of cultured cancer cells was significantly less than SN38.[34] These findings suggest that PEG-S-S-SN38 NPs possess better *in vitro* anticancer activity than OEG-SN38 NPs, which might be attributed to the promoted release of SN38 from PEG-S-S-SN38 NPs due to the multi-stimuli responsiveness. Compared with the control groups, CPT-11 did not cause obvious in the cell cycle distribution at both time points. These findings coincide with the fact that CPT-11 has little or no anticancer activity *in vitro*, and

View Article Online
DOI: 10.1039/C6TB02262F

needs to be converted into active metabolite SN38 to exhibit therapeutic activity.

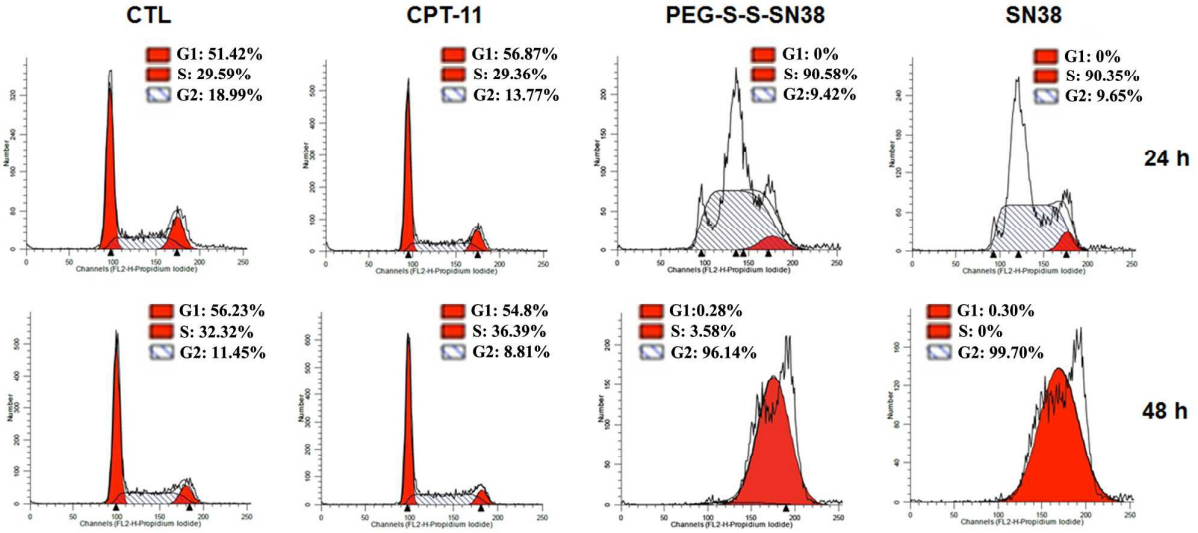

Figure 4. Cell cycle distribution and regulation. BCap37 cells treated with CPT-11, SN38 and PEG-S-S-SN38 at a concentration equivalent to 0.04 μg mL^{-1} SN38 for 24 h and 48 h, respectively, were monitored by flow cytometric analysis.

In vivo antitumor activity of CPT-11 and PEG-S-S-SN38 NPs

All animal studies were performed in strict accordance with Chinese legislation on the use and the care of laboratory animals, and with the guidelines established by the Institute for Experimental Animals. To evaluate their *in vivo* antitumor activity, PEG-S-S-SN38 NPs and CPT-11 were administered intravenously *via* tail vein at a dosage equivalent to 10 mg kg^{-1} SN38 in nude mice bearing BCap37 xenograft tumors for a total of 6 cycles (Figure 5). Our data showed that both treatment significantly repressed the tumor growth (P<0.0005 for CPT-11 *vs* PBS; P<0.00005 for PEG-S-S-SN38 *vs* PBS). Meanwhile, the IR (inhibition rate of tumor growth) induced by PEG-S-S-SN38 NPs reached 72.49% ± 6.26%, which is nearly double that of CPT-11 (IR=38.64% ± 13.04%)(Figure 5A, 5C and 5D, P<0.0005 for PEG-S-S-SN38 *vs* CPT-11). In addition, neither CPT-11 nor PEG-S-S-SN38 NPs induced significant changes on body weight in comparison with the control group (Figure 5B). These data indicate that PEG-S-S-SN38 NPs possess not only excellent *in vivo* safety, but much better therapeutic efficacy than CPT-11 at equivalent dosage. Moreo-

View Article Online
DOI: 10.1039/C6TB02262F

ver, in a preliminary study examining the drug distribution in different organs/tissues of mice bearing BCap37 xenograft tumors, we found that similar to many other nano-DDSs, PEG-S-S-SN38 NPs were mainly cleared by liver and spleen (Figure S8).

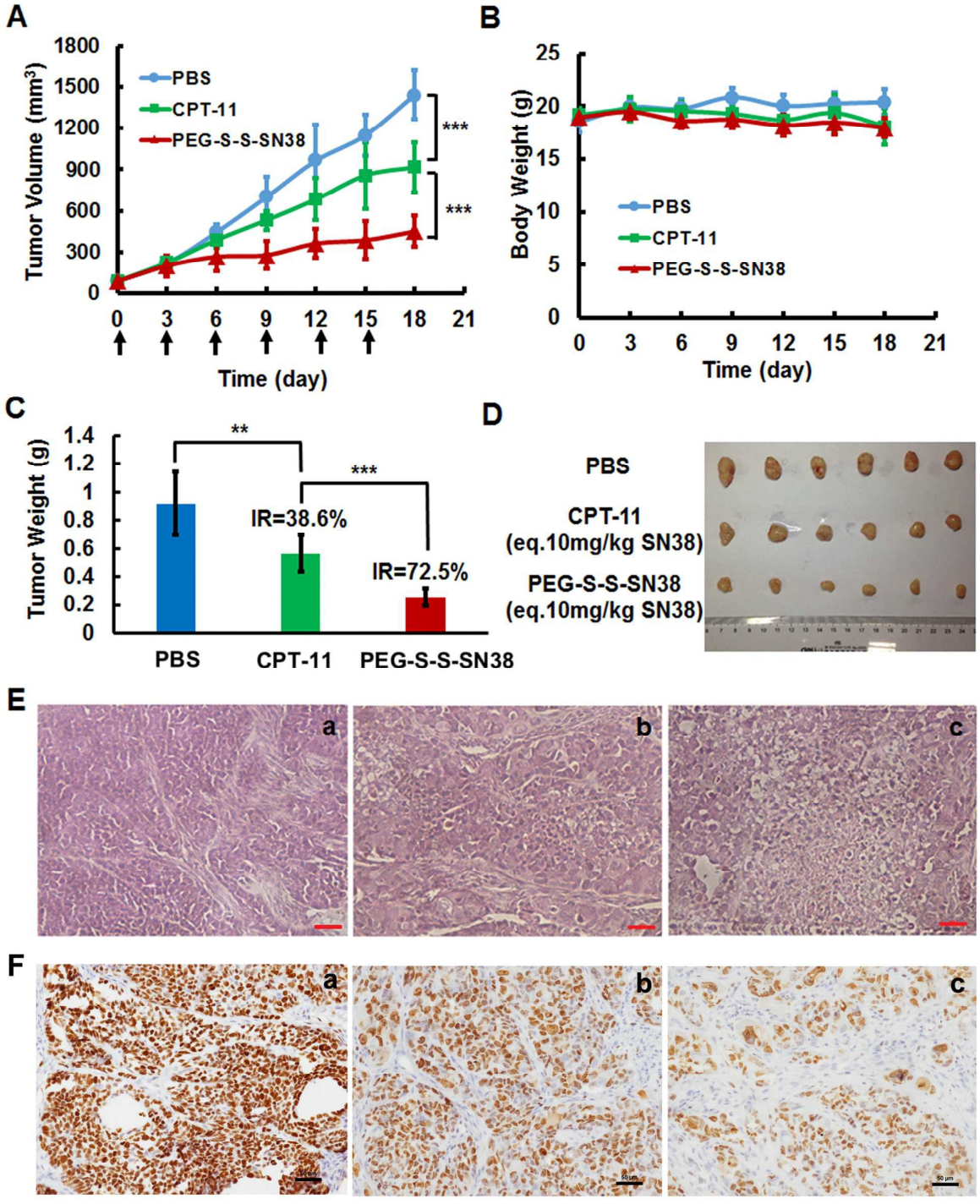

Figure 5. *In vivo* therapeutic effects of CPT-11 and PEG-S-S-SN38 against BCap37 human breast xenograft tumors. (A) Changes in tumor volume. (B) Body weight changes of the nude mice. (C) The average tumor weight of

View Article Online
DOI: 10.1039/C6TB02262F

each group at the end of experiment; IR, the inhibition rate of tumor growth. (D) Photos of xenograft tumors at the termination of animal experiment. (E) and (F) Representative histological and Ki-67 immunohistochemical features of tumor tissues; a) PBS group, b) CPT-11 group, c) PEG-S-S-SN38 group. $^{**}P<0.005$, and $^{***}P<0.0005$. Scale bars: 100 μm for E; 50 μm for F.

Histological studies and immunohistochemical staining of proliferation marker Ki-67 with xenograft tumors further confirmed the therapeutic superiority of PEG-S-S-SN38 NPs over CPT-11. In H&E staining, the tumor tissues were composed of tightly packed tumor cells and stroma in the control group, while apoptotic cell death were observed in a small portion of tumor cells in tissue sections obtained from CPT-11 group, which was characterized by membrane-bound, small nuclear fragments surrounded with a rim of cytoplasm. However, in xenograft tumors treated with PEG-S-S-SN38 NPs, nearly all the tumor cells exhibited typical apoptotic features and even obvious vacuolization was observed (Figure 5E). Moreover, administration of CPT-11 and PEG-S-S-SN38 NPs significantly reduced both the percentage of Ki-67 positive-cells and the expression level of Ki-67, especially in PEG-S-S-SN38-treated tumors (Figure 5F). These data also demonstrated that consistent with their better activity in inducing cell cycle arrest *in vitro* (see above section), PEG-S-S-SN38 NPs exhibit significantly increased *in vivo* anticancer activity compared with OEG-SN38 NPs, as the latter only achieved anticancer activity comparable to CPT-11 against BCap37 xenograft tumors.[34]

Conclusions

Dual and multi-stimuli responsive drug delivery systems hold the promise to further improve the performances of DDS. In the present study, we successfully synthesized a novel SN38 prodrug PEG-S-S-SN38, for the first time, through conjugating PEG and SN38 with both disulfide bond and carbonic ester linkage as the linkers for efficient delivery of SN38. The amphiphilic PEG-S-S-SN38 has a high SN38 loading content and could self-assemble into nanoparticles with a stable diameter

View Article Online
DOI: 10.1039/C6TB02262F

of about 73 nm. These nanoparticles have no initial burst release, but exhibit favorable stimuli-responsiveness to GSH, esterase and H_2O_2 for the controlled release of SN38. Most importantly, PEG-S-S-SN38 NPs possess excellent *in vitro* anticancer activity comparable to free SN38, and show dramatically increased *in vivo* anticancer activity compared with both the corresponding clinical chemotherapy drug CPT-11 and OEG-SN38 NPs previously reported. Our data suggest that the responsiveness of PEG-S-S-SN38 NPs to a combination of three stimulus remarkably enhances their therapeutic activity against heterogeneous or mixed cell population in tumors, making this new DDS a promising alternative of CPT-11 for cancer treatment.

Acknowledgements

This work was supported by the National Natural Science Foundation of China (NSFC 21104065, 21274125 and 21574118) and the Zhejiang Provincial Natural Science Foundation for Distinguished Young Scientists (No. LR16H160002).

References

1 M. E. Davis, Z. Chen and D. M. Shin, *Nat. Rev. Drug Discovery*, 2008, **7**, 771.

2 R. T. Sadikot, *Adv. Drug Delivery Rev.*, 2014, **77**, 27.

3 H. Maeda and Y. Matsumura, *Adv. Drug Delivery Rev.*, 2011, **63**, 129.

4 V. P. Torchilin, *Nat. Rev. Drug Discovery*, 2014, **13**, 813.

5 G. G. Chabot, *Clin. Pharmacokinet.*, 1997, **33**, 245.

6 Y. Sadzuka, H. Takabe and T. Sonobe, *J. Controlled Release*, 2005, **108**, 453.

7 H. C. Pitot, A. A. Adjei, J. M. Reid, J. A. Sloan, P. J. Atherton, J. Rubin, S. R. Alberts, B. A. Duncan, L. Denis, L. J. Schaaf, D. Yin, A. Sharma, P. McGovren, L. L. Miller and C. Erlichman, *Cancer Chemother. Pharmacol.*, 2006, **58**, 165.

8 N. F. Smith, W. D. Figg and A. Sparreboom, *Toxicol. In Vitro*, 2006, **20**, 163.

9 F. Innocenti, D. L. Kroetz, E. Schuetz, M. E. Dolan, J. Ramirez, M. Relling, P. Chen, S. Das, G. L. Rosner and M. J. Ratain, *J. Clin. Oncol.*, 2009, **27**, 2604.

View Article Online
DOI: 10.1039/C6TB02262F

10 H. Bleiberg, *Eur. J. Cancer*, 1999, **35**, 371.

11 A. Pal, S. Khan, Y. F. Wang, N. Kamath, A. K. Sarkar, A. Ahmad, S. Sheikh, S. Ali, D. Carbonaro, A. Zhang and I. Ahmad, *Anticancer Res.,* 2005, **25**, 331.

12 N. Vijayalakshmi, A. Ray, A. Malugin and H. Ghandehari, *Bioconjugate Chem.*, 2010, **21**, 1804.

13 Y. Matsumura, *Adv. Drug Delivery Rev.*, 2011, **63**, 184.

14 V. Bala, S. Rao, B. J. Boyd and C. A. Prestidge, *J. Controlled Release*, 2013, **172**, 48.

15 P. Sapra, H. Zhao, M. Mehlig, J. Malaby, P. Kraft, C. Longley, L. M. Greenberger and I. D. Horak, *Clin. Cancer Res.*, 2008, **14**, 1888.

16 R. Cheng, F. Meng, C. Deng, H. A. Klok and Z. Zhong, *Biomaterials*, 2013, **34**, 3647.

17 S. Ganta, H. Devalapally, A. Shahiwala and M. Amiji, *J. Controlled Release*, 2008, **126**, 187.

18 N. Rapoport, *Prog. Polym. Sci.*, 2007, **32**, 962.

19 F. H. Meng, Z. Y. Zhong and J. Feijen, *Biomacromolecules*, 2009, **10**, 197.

20 R. Cheng, F. Feng, F. Meng, C. Deng, J. Feijen and Z. Zhong, *J. Controlled Release*, 2011, **152**, 2.

21 F. H. Meng, W. E. Hennink and Z. Zhong, *Biomaterials*, 2009, **30**, 2180.

22 P. Kuppusamy, H. Q. Li, G. Ilangovan, A. J. Cardounel, J. L. Zweier, K. Yamada, M. C. Krishna and J. B. Mitchell, *Cancer Res.*, 2002, **62**, 307.

23 H. Wei, R.-X. Zhuo and X.-Z. Zhang, *Prog. Polym. Sci.*, 2013, **38**, 503.

24 R. Cheng, F. Meng, C. Deng, H.-A. Klok and Z. Zhong, *Biomaterials*, 2013, **34**, 3647.

25 Y. C. Wang, F. Wang, T. M. Sun and J. Wang, *Bioconjugate Chem.*, 2011, **22**, 1939.

26 J.-H. Ryu, R. Roy, J. Ventura and S. Thayumanavan, *Langmuir*, 2010, **26**, 7086.

27 Z.-Y. Qiao, R. Zhang, F.-S. Du, D.-H. Liang and Z.-C. Li, *J. Controlled Release*, 2011, **152**, 57.

28 Z. Jia, L. Wong, T. P. Davis and V. Bulmus, *Biomacromolecules*, 2008, **9**, 3106.

29 X.-Q. Li, H.-Y. Wen, H.-Q. Dong, W.-M. Xue, G. M. Pauletti, X.-J. Cai, W.-J. Xia, D. Shi and Y.-Y. Li, *Chem. Commun.*, 2011, **47**, 8647.

30 I. Rosenbaum, A. J. Harnoy, E. Tirosh, M. Buzhor, M. Segal, L. Frid, R. Shaharabani, R. Avinery, R. Beck and R. J. Amir, *J. Am. Chem. Soc.*, 2015, **137**, 2276.

31 J. Rao, C. Hottinger and A. Khan, *J. Am. Chem. Soc.*, 2014, **136**, 5872.

32 J. Wang, X. Sun, W. Mao, W. Sun, J. Tang, M. Sui and Y. Shen, Z. Gu, *Adv. Mater.*, 2013, **25**, 3670.

33 Y. Q. Shen, E. L. Jin, B. Zhang, C. J. Murphy, M. H. Sui, J. Zhao, J. Q. Wang, J. B. Tang, M. H. Fan, E. Van

View Article Online
DOI: 10.1039/C6TB02262F

Kirk and W. J. Murdoch, *J. Am. Chem. Soc.*, 2010, **132**, 4259.

34 H. Zhang, J. Wang, W. Mao, J. Huang, X. Wu, Y. Shen and M. Sui, *J. Controlled Release*, 2013, **166**, 147.

35 P. F. Gou, W. W. Liu, W. W. Mao, J. B. Tang, Y. Q. Shen and M. H. Sui, *J. Mater. Chem. B*, 2013, **1**, 284.

36 K. Knop, R. Hoogenboom, D. Fischer and U. S. Schubert, *Angew. Chem. Int. Ed.*, 2010, **49**, 6288.